Geologia Croatica	67/1	17–32	10 Figs.	4 Tabs.		Zagreb 2014

Geochemistry of the Görcsöny Ridge amphibolites (Tisza Unit, SW Hungary) and its geodynamic consequences

Tivadar M. Tóth

Department of Mineralogy, Geochemistry, and Petrology, University of Szeged
H-6722 Szeged, Egyetem u. 2-6, Hungary; (mtoth@geo.u-szeged.hu)

doi: 10.4154/gc.2014.02

Geologia Croatica

ABSTRACT

The Görcsöny Ridge is part of the complicated Variscan metamorphic basement of the SW Tisza plate. It was penetrated by several wells, one of which (Baksa-2) has 1200 m of well core available for petrological examination. Amphibolite samples of this core are of two different sorts: the first group contains biotite, rutile, and garnet, while the second group contains ilmenite and is free of garnet. The two rock types occur separately in the borehole, defining a lower and an upper unit (LU, UU). Based on their major and trace element compositions, LU samples represent within-plate (WP) tholeiites which assimilated pelagic sediments, while those of the UU represent WP alkali basalts. Thermobarometric calculations suggest that the difference in chemical composition itself does not explain the above differences in mineralogy, so the two units must also differ in their metamorphic histories. Consequently, the crystalline basement of the Görcsöny Ridge possibly consists of amalgamated fragments of different origins which became juxtaposed during the Variscan collisional orogeny.

Keywords: Tisza plate, Variscan orogeny, amphibolite geochemistry

1. INTRODUCTION

The Tisza Unit (e.g. CSONTOS et al., 1992) is a microcontinent which represents the European margin of Tethys and reached its present location through horizontal microplate displacement during the Alpine orogenic cycle. Although Palaeozoic and Mesozoic sedimentary facies zones which cover the crystalline basement show a good correlation with those recognized in different Tethian realms, (HAAS et al., 1995, and references therein), there are still many open questions concerning the relationships between the underlying crystalline rocks of the European Variscan Belt and those of the Tisza plate. Granitoid rocks of the SW part of the Tisza Unit (Mórágy Complex) were found to be similar to the rocks of the Central Bohemian Massif, based on petrological and geochemical studies (BUDA, 1981) as well as age constraints (KLÖTZLI et al., 2004). According to SZEDERKÉNYI (1996), eclogite samples from the NE and SW part of the Tisza Unit represent a SW–NE trending suture zone of an ancient Variscan ocean. SZEDERKÉNYI (1996) suggested a possible geological relationship between the low grade Silurian black shales in the SW part of the Tisza and those in the Moravicum. If all these ideas fit, the Tisza Unit should represent a composite segment of diverse tectonic realms of the European Variscan Belt. Although at present correlating the evolution of the Tisza basement with that of the European Variscan belt is only a theoretical possibility, PAMIĆ et al. (2002) and BALEN et al. (2006) call attention to the close relationship between the basement of the Görcsöny Ridge inside the Tisza plate and the Slavonian Mountains in Croatia. They also offer a detailed evaluation of the geochemical and petrological data of diverse amphibolite types.

The Görcsöny Ridge is located in the SW part of the Tisza Unit (Fig. 1) bordered by tectonic lines in each direction. Several boreholes penetrated the crystalline basement beneath the Neogene clastic sediments, among which the

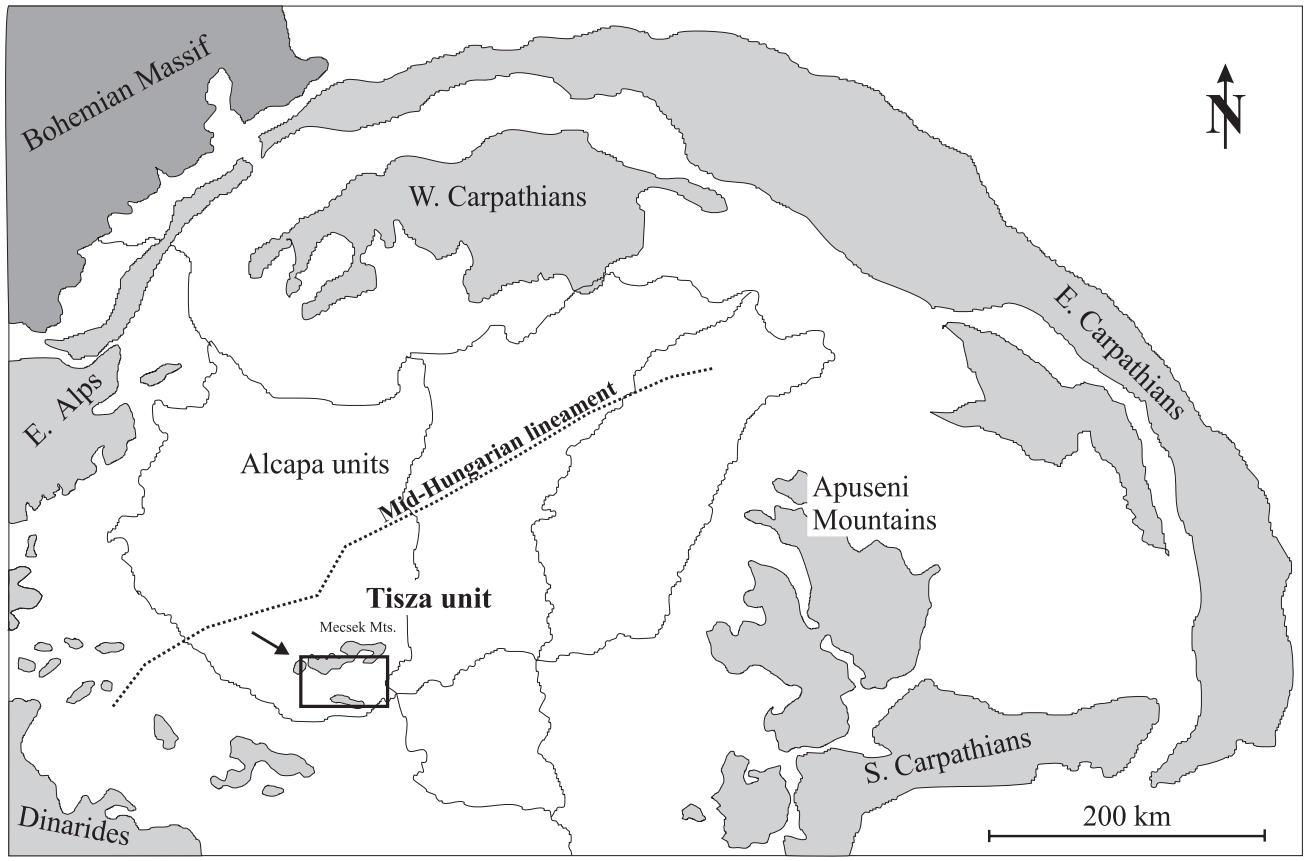

Figure 1: Tectonic sketch map of the Tisza Unit in the Alpine-Carpathian-Pannonian framework. The arrow points to the study area.

deepest is the Baksa-2 well, which has a total thickness of 1200 m and a core recovery close to 100%. The most common rock types throughout the Görcsöny Ridge are different kinds of gneiss and mica schist, marble, calc-silicate rocks, and amphibolite. Additionally, one eclogite sample has been described by RAVASZ-BARANYAI (1969), while eclogite pebbles in the overlying Miocene conglomerate were reported by HORVÁTH et al. (2003). Among the many rock bodies, which show a significant positive magnetic anomaly, one has been exposed by a borehole and was proven to be a partially serpentinized ultramafic body (Gyód serpentinite, BALLA, 1983; SZEDERKÉNYI, 1974; KOVÁCS et al., 2009).

Geochemical features of the amphibolite and eclogite samples throughout the Görcsöny Ridge were discussed by SZEDERKÉNYI (1983), who found them to be similar to mid-ocean ridge basalt (MORB) tholeiites. The parent rock of gneiss and micaschist is thought to be a greywacke type sediment (SZEDERKÉNYI, 1977). Geochemical and thermobarometric data prove that the protolith of the serpentinite body is of harzburgite composition, representing an oceanic upper mantle source (~1100 °C, 8.5 kbar, KOVÁCS et al., 2009). For the Görcsöny Complex gneiss and mica schist, SZEDERKÉNYI (1976) suggested a polyphase metamorphic evolution with five subsequent events, which was later simplified by ÁRKAI (1984) and ÁRKAI et al. (1985, 1999). For the earliest Barrovian event they calculated a T_{max} of about 660 ± 25 °C at 7.5 ± 0.5 kbar pressure followed by an isothermal decompression down to 4.4 ± 0.2 kbar at 650 ± 40 °C. This evolution seems to be typical for a significant part of the study area. The metamorphic history of the only known Gyód serpentinite body is only partly similar, exhibiting a continuous retrograde pathway and hydration with significant recrystallization at ~650 °C and 4 kbar and serpentinization at ~250 °C (KOVÁCS et al., 2009). The appearance of post-kinematic antigorite and talc suggests a late reheating event, totally unknown from the surrounding gneiss terrain. As a consequence, serpentinite must represent a foreign tectonic regime inside the Görcsöny Complex. Similarly, the only eclogite sample of the Görcsöny-1 well suggests an exotic origin. Recently, NAGY & TÓTH (2009) called attention to the importance of textural relics in the lowermost section of the Baksa-2 borehole, suggesting a significantly different metamorphic evolution in the upper and lower segments of the Görcsöny Ridge metamorphic block. All available data of the Görcsöny Complex represent Variscan cooling ages (K/Ar in amphibole and biotite, Rb/Sr in biotite, Ar/Ar in muscovite) for the amphibolite-facies metamorphic rocks (summarized in LELKES-FELVÁRI & FRANK, 2006 and references therein).

To be able to correlate the Görcsöny Complex with other parts of the Tisza Unit and also with other segments of the European Variscan Belt, diverse geochemical, petrological and geochronological data must be considered. The aim of this study is to specify the chemical composition of the amphibolites in the Görcsöny Complex. In addition to the data

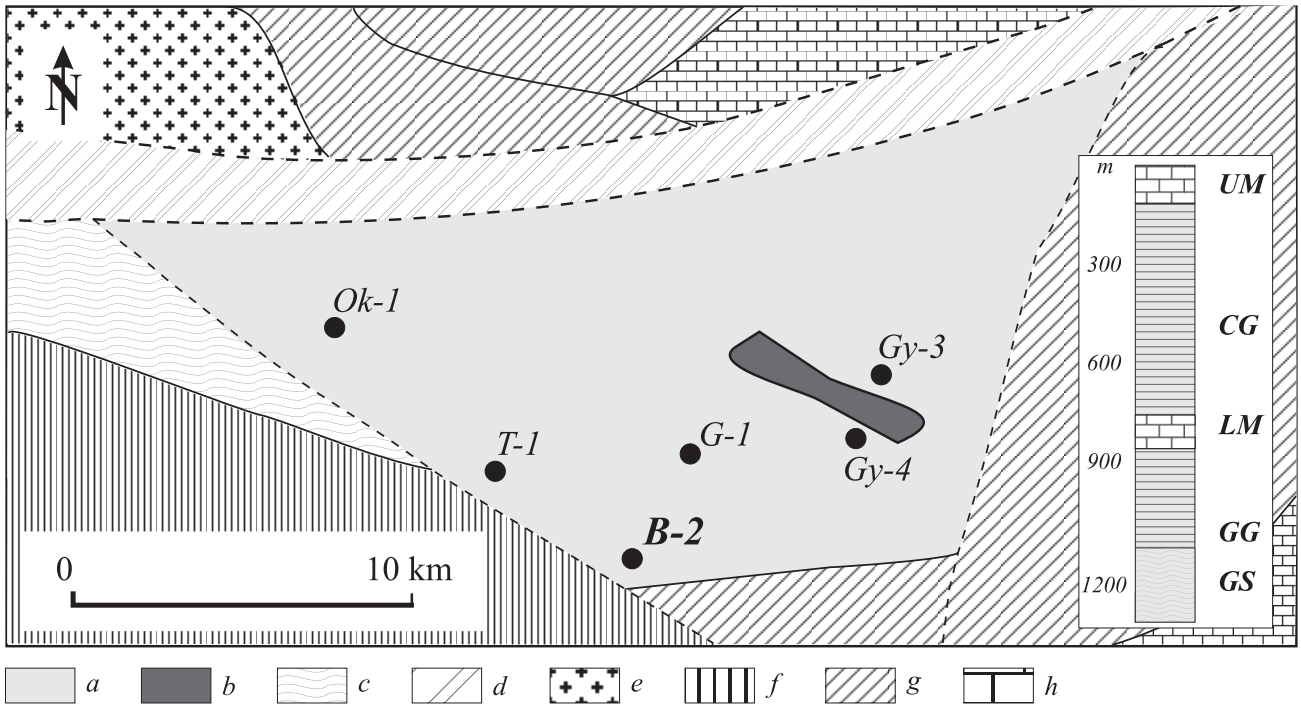

Figure 2: A simplified tectonic map of the pre-Neogene basement of southern Transdanubia (after FÜLÖP, 1994). a) Görcsöny Complex, b) Gyód serpentinite, c) Görgeteg Complex, d) Ófalu phyllite, e) Mórágy granite, f) Carboniferous molasse, g) Permian sandstone, h) Triassic carbonates. Inset: Rock units of the Baksa-2 well. UM: upper marble; CG: chloritic gneiss; LM: lower marble; GG: garnetiferous gneiss; GS: garnetiferous mica schist.

available so far (collected by SZEDERKÉNYI, 1983), the results of 34 new major and trace element measurements are included. As a result, the data of all known amphibolite bodies are included in the dataset even if some samples (no longer available) are represented only by their historical measurements. Given the still obscure tectonic relationships, amphibolite data of the neighbouring units, Mórágy Granite Complex (ÁRKAI & NAGY, 1994) and Ófalu phyllite zone, are disregarded in this study.

2. GEOLOGICAL SETTING

The crystalline basement of the SW part of the Tisza Unit is a complicated puzzle of blocks with incoherent metamorphic evolution histories (Fig. 2). In the north, the Görcsöny Ridge is bordered by the Ófalu phyllite zone, where various low grade rocks occur. To the east and northwest the Görcsöny Ridge is separated from the large anatectic granitoid body of the Mórágy Complex (BALLA & GYALOG, 2009, and references therein). Although there are essential petrological data that suggest a similar evolution (HORVÁTH et al., 2010), no direct information is available on the relationship between the Görcsöny Complex and the crystalline basement of northern Croatia to the south because of the thick sedimentary cover. According to ÁRKAI (1984), the metamorphic evolution of the Görgeteg-Babócsa basement in the west is identical to that of the Görcsöny Complex, although their petrography differs slightly. Based on the very sporadic information, the lithology of the western part is less complicated, consisting exclusively of gneiss and mica schist.

The type locality of the study area is the Baksa-2 well, which has been subdivided into five downward successions based on the dominant rock types. These are the "upper marble", "chloritic two-mica gneiss", "lower marble", "garnetiferous two-mica gneiss", and "garnetiferous two-mica schist" units (KOVÁCH et al., 1985, Fig. 2 inset). In addition to marble, carbonate units also contain different calc-silicate rocks with tremolite, diopside, epidote, and garnet. In the gneiss and mica schist samples, garnet, staurolite, kyanite, and sillimanite are common; they usually contain a large amount of graphite (SZEDERKÉNYI, 1996).

Amphibolite bodies of different thicknesses appear concentrated in three sections along the well. Numerous thin (up to about 50 cm) horizons appear between 830 and 870 m. At greater depths, within the lowermost units, two swarms of amphibolite occur in the 1020–1060 and 1130–1160 m intervals, respectively (Fig. 2 inset). Amphibole-plagioclase as well as amphibole-garnet thermobarometric calculations resulted in slightly different peak conditions for the different samples (550–690 °C at 4–5.5 kbar, ÁRKAI et al., 1999; 550–650 °C at 5–7 kbar, KIRÁLY, 1996). Although only one eclogite sample has been reported from the crystalline basement itself (RAVASZ-BARANYAI, 1969), there are many eclogite pebbles in the overlying clastic sediments (HORVÁTH et al., 2003; LELKES-FELVÁRI GY. pers. comm.). The garnet amphibolite of the Gy-3 well, like the eclogite, suggests a high dP/dT metamorphic peak: 7.5 kbar at 480 °C (KIRÁLY, 1996). Textural relicts mostly appear as inclusions in large garnet grains of the garnetiferous two-mica gneiss and schist units, and were studied in detail by NAGY & TÓTH (2009). Among the common inclusions of quartz and ilmenite, kyanite as well as plagioclase, K-feldspar, apatite, and biotite grains of special appearance are observed. Feld-

spar and apatite inclusions are usually faceted and have radial cracks around them, suggesting significant decompression during the metamorphic history (VAN DER MOLEN and VAN ROERMUND, 1986). Biotite exhibits symplectic intergrowth with worm-like quartz and rutile. Thermobarometric calculations prove an early event of $T \sim 680–720$ °C and $P \sim 8–9$ kbar based on these inclusions. This metamorphic event is absolutely unknown from the upper units of the Baksa-2 well.

Post-metamorphic palaeofluid evolution of the Görcsöny Complex was governed by two main subsequent events based on evaluation of the veins crosscutting the gneiss body (FINTOR et al., 2008, 2010, 2011). The early propylitic veins are characterized by the presence of diopside, epidote, and polymetallic ore minerals, pyrite, chalcopyrite, pyrrhotite, galena, and sphalerite (TARNAI, 1997, 1998). This paragenesis formed in a wide temperature interval decreasing from 480 down to ~150 °C. Late quartz-carbonate veins crystallized from a low temperature (130–60 °C) hypersaline fluid. Although the presence of this second vein generation is common across the whole area, including the Permo-Carboniferous sedimentary cover formations (FINTOR et al., 2009), propylitic veins occur exclusively in the uppermost three units.

All previous results considered, there are remarkable differences in the metamorphic and post-metamorphic evolution of the upper and lower segments of the studied well and probably also in different realms of the Görcsöny Complex. The two blocks are now referred to here as the upper unit (UU) and the lower unit (LU).

3. ANALYTICAL METHODS

Whole rock compositions of 34 amphibolite samples were measured using an automated Philips PW1453 X-ray fluorescence spectrometer with a Sc-Mo tube at the XRF laboratory of the University of Fribourg (Switzerland). Major elements were determined from fusion discs fused in a Pt crucible at 1000 ºC. The following trace elements were measured in pressed disks: V, Cr, Ni, Ga, Zr, Y, Nb, Rb, Sr, and Ba. Natural standards were used for the measurements. Both major and trace element data have a relative precision better than 2%. Historical geochemical data are collected in SZEDERKÉNYI (1983).

Electron microprobe measurements were performed at the Montanuniversität, Leoben, in Austria using ARL-SEMQ 30 equipment with 15 kV accelerating voltage and 12 nA

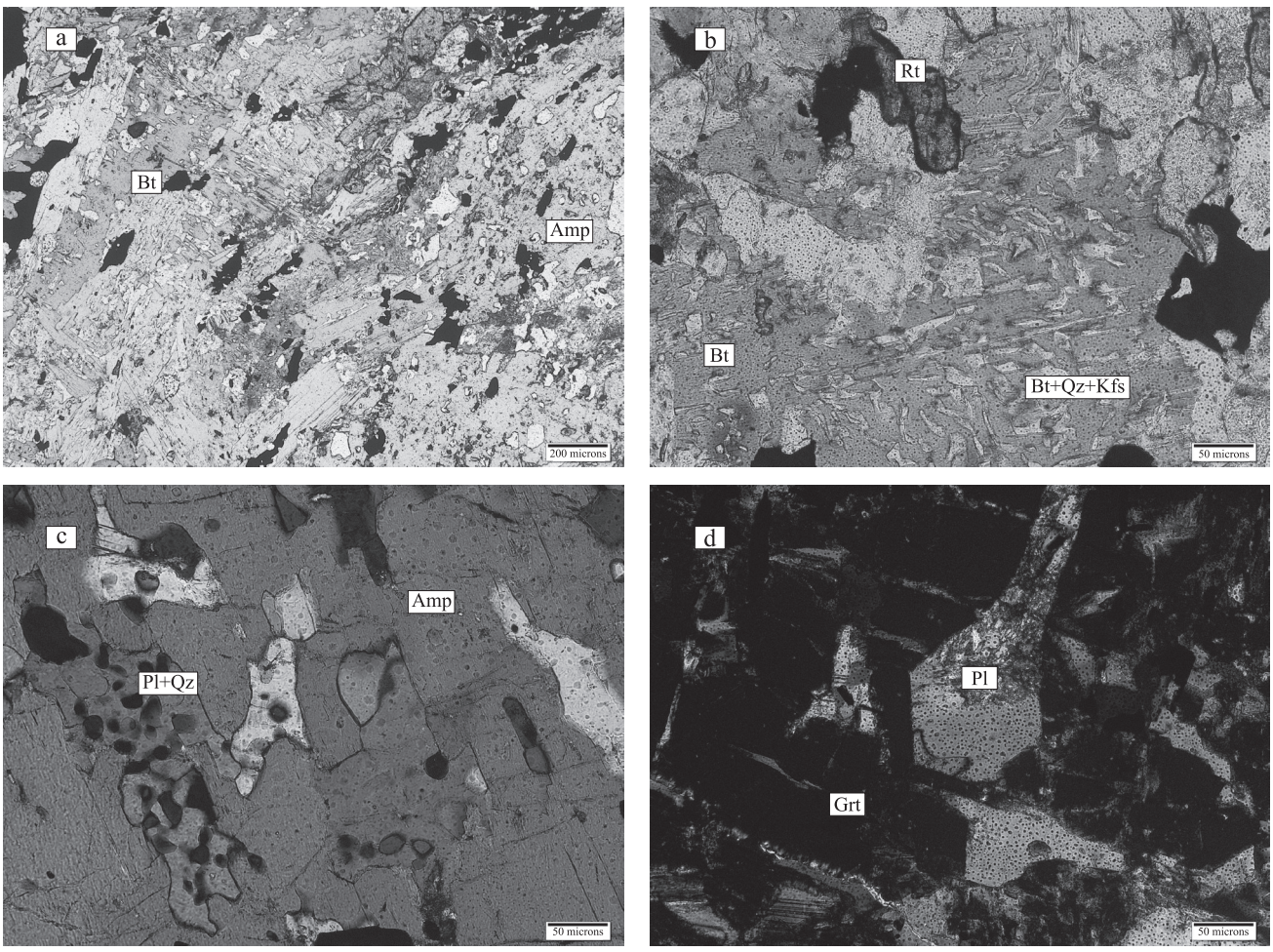

Figure 3: Thin section photo micrographs of relic textures of the LU amphibolites. a) Mica-rich band with symplectitic biotite grains (+N). b) Fine-grained biotite+quartz symplectite of the LU amphibolite (+N). c) Calcic myrmekite inclusions in amphibole (+N). d) Plagioclase inclusions in garnet usually have faceted habit (+N).

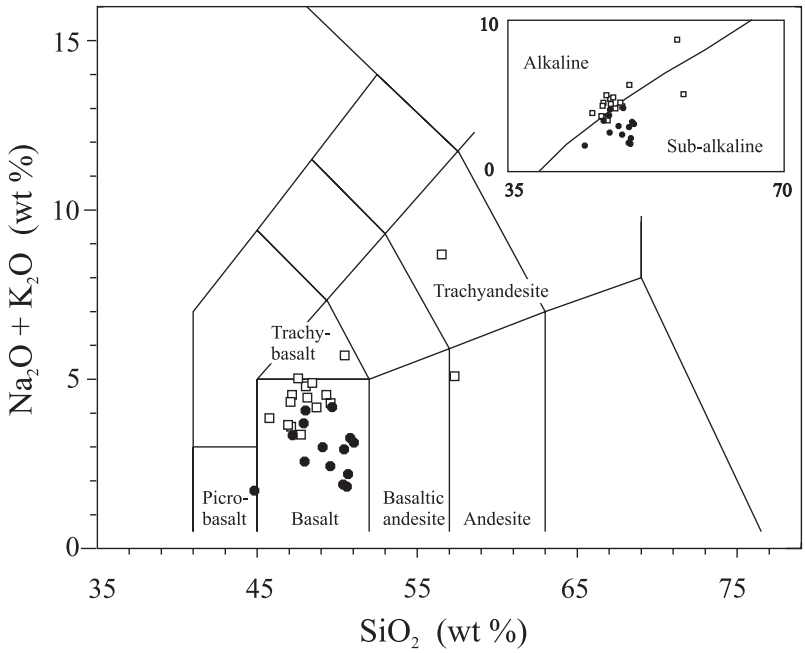

Figure 4: Amphibolite samples of the two units in the TAS diagram (LE MAITRE, 1989) suggest different compositions. Inset: the alkaline-subalkaline discrimination after IRVINE & BARAGAR, 1971. Squares: UU; dots: LU.

sample current. Counting times of 20 s for Si, Al, Mg, Ca and K, and 30 s for Fe, Na, Mn and Ti were applied. For standardization, synthetic and natural mineral standards were used. The analytical error of the microprobe for the main elements (>10 m/m%) is less than 1%; for main and minor elements (2–10 m/m%) it is about 2%.

4. RESULTS

4.1. Petrography

4.1.1. Amphibolite

At first sight, there are two distinct types of amphibole-bearing rocks in the Baksa-2 borehole. In the upper marble unit, calc-silicate rock samples occur, which contain varying amounts of amphibole due to their different chemical bulk compositions as well as the P, T, and X_{CO2} conditions during the metamorphic evolution. These samples have, without doubt, a sedimentary protolith, and have therefore been disregarded in the following study, which, instead, is focused on the rocks with magmatic origin.

Orthoamphibolite becomes an essential rock type below ~800 m in the Baksa-2 borehole. The samples are massive, and in a few cases also foliated. They are dark green in colour and consist basically of hornblende with various amount of plagioclase. Other constituents (quartz, garnet, biotite, and the Ti-phases) occur in subordinate amounts. The mineralogical composition and textural features of the amphibolites change abruptly at the top of the garnetiferous two-mica gneiss unit (870 m, see inset of Fig. 2). In the upper segment, medium grained, equilibrium texture amphibolite is common; relict mineral grains or textures are not observed. Amphibole is normal hornblende; the prevailing Ti-mineral is ilmenite, usually surrounded by titanite. The rock samples contain significantly more plagioclase than the samples of the lower segment of the well, while garnet, rutile, and biotite are entirely absent.

In contrast, in amphibolite intercalations of the garnetiferous two-mica gneiss, relict mineral grains and textural domains have also been preserved. Below about 1020 m the main Ti-phase is rutile, usually mantled by ilmenite. Within the 150 m interval between the two well-defined depths no amphibolite is present, making the exact specification of the border problematic. In the rutile-bearing part, garnet also appears in most samples, in general having a resorbed appearance and containing many rutile inclusions. Garnet occasionally also occurs as an inclusion in the large amphibole grains. Most amphibolite samples contain various amounts of biotite. In these mica-rich bands of the rock a fine-grained symplectite of biotite, quartz, and K-feldspar is common (Fig. 3a, b). In addition to feldspar grains in textural equilibrium with amphibole, relict plagioclase occurs both as a matrix constituent and as an inclusion in amphibole and garnet. These sets of idioblastic plagioclase grains regularly form polygonal texture, and several crystals appear in vermicular intergrowth with quartz forming calcic myrmekite (Fig. 3c) (DYMEK & SCHIFFRIES, 1987). Feldspar inclusions in garnet are usually faceted with common radial cracks at the crystal edges (Fig. 3d).

The abrupt change in amphibolite mineralogy and textures between the upper and lower units may be the result of a drastic change in either the bulk chemical composition or the metamorphic history of the two parts or both.

4.2. Geochemistry

Although the chemical compositions of amphibolites may be significantly different from their parent igneous equivalents due to post-magmatic processes, these data sets are

Table 1: Chemical compositions of the amphibolite samples studied (oxides in m/m%, trace elements in ppm).

Unit	UU	UU	UU	UU	UU	UU	UU	UU	UU	UU	UU	UU
Sample	B2-680	B2-681	B2-699	B2-701	B2-702	B2-703	B2-704	B2-706	B2-707	B2-708	B2-709	B2-711
Depth	827 m	829 m	846 m	850 m	853 m	854 m	854 m	857 m	859 m	861 m	864 m	866 m
SiO_2	49.09	48.88	47.22	46.24	47.13	47.49	50.43	48.15	46.67	47.49	46.48	44.73
TiO_2	3.17	3.29	2.62	2.75	3.81	4.26	2.92	3.01	3.14	2.86	3.34	3.76
Al_2O_3	13.42	14.08	11.65	12.80	14.46	14.83	13.81	14.48	14.34	14.59	13.92	14.70
$Fe_2O_3^{tot}$	11.78	11.65	13.49	14.33	12.14	14.19	13.69	13.47	13.84	12.74	13.22	15.85
MnO	0.30	0.19	0.21	0.23	0.18	0.23	0.23	0.20	0.18	0.18	0.18	0.23
MgO	6.25	6.45	8.75	7.63	4.31	4.76	3.51	6.58	4.85	6.59	6.19	5.36
CaO	10.36	9.67	11.27	10.64	11.01	8.61	8.72	8.32	10.94	9.51	10.67	8.67
Na_2O	3.10	3.18	2.51	2.61	4.13	4.15	5.20	3.69	3.25	3.55	3.07	3.34
K_2O	1.15	1.32	0.82	0.99	0.57	0.87	0.50	1.17	1.24	0.85	1.21	0.43
P_2O_5	0.38	0.39	0.39	0.33	0.39	0.46	0.92	0.35	0.47	0.32	0.45	0.66
LOI	1.22	1.32	1.19	1.06	1.68	0.62	0.36	0.89	1.02	1.01	1.17	2.68
Total	100.21	100.40	100.12	99.61	99.81	100.45	100.29	100.32	99.93	99.72	99.89	100.41
Cr	93	94	188	132	14	9	15	92	43	101	147	80
Ni	79	62	97	89	15	11	1	65	30	66	65	31
V	398	428	342	396	403	421	174	372	397	378	409	381
Rb	80	81	30	37	13	25	2	32	54	21	41	22
Sr	433	492	235	305	450	511	416	553	429	430	426	491
Ba	171	263	165	148	111	137	92	254	215	138	226	70
Ga	18	21	15	19	26	25	24	22	22	21	21	33
Nb	31	31	24	25	32	39	65	29	34	29	37	45
Y	31	31	23	27	29	34	61	27	36	28	33	41
Zr	186	190	148	141	184	223	400	193	213	174	206	238
Unit	LU	LU	LU	LU	LU	LU	LU	LU	LU	LU	LU	LU
Sample	B2-803	B2-804	B2-810	B2-811	B2-816	B2-828	B2-832	B2-833	B2-889	B2-907	B2-911	B2-913
Depth	1020 m	1022 m	1035 m	1036 m	1044 m	1062 m	1066 m	1067 m	1128 m	1150 m	1152 m	1153 m
SiO_2	55.59	50.07	49.95	49.84	43.65	50.06	47.87	50.43	48.98	49.74	47.45	48.78
TiO_2	1.40	2.10	3.83	0.86	3.62	2.94	2.68	2.72	2.11	2.82	3.07	3.75
Al_2O_3	18.15	14.78	14.16	10.55	10.68	11.14	14.43	14.68	15.44	17.37	16.24	14.27
$Fe_2O_3^{tot}$	8.27	11.69	14.21	12.25	14.74	13.22	12.03	12.59	12.99	11.75	12.24	13.75
MnO	0.06	0.15	0.19	0.18	0.15	0.17	0.16	0.19	0.21	0.19	0.22	0.27
MgO	4.49	8.44	4.73	12.87	8.03	9.62	6.66	6.74	7.38	3.64	5.25	5.28
CaO	3.89	7.55	8.31	10.04	14.10	9.08	8.12	8.27	9.02	10.87	11.23	10.08
Na_2O	3.20	0.68	1.31	0.83	0.89	0.88	2.23	2.27	1.39	0.99	1.09	1.94
K_2O	1.74	2.39	1.59	0.97	0.78	1.29	1.80	0.97	1.02	0.88	1.45	1.04
P_2O_5	0.18	0.24	0.76	0.10	0.75	0.39	0.37	0.40	0.28	0.48	0.69	0.21
LOI	3.05	2.26	1.25	1.86	2.27	1.65	3.45	1.07	1.62	1.29	1.33	0.77
Total	100.01	100.35	100.28	100.36	99.65	100.44	99.82	100.34	100.44	100.01	100.25	100.13
Cr	136	349	28	598	483	615	165	149	201	60	86	32
Ni	44	84	25	477	417	188	93	90	74	33	47	6
V	257	298	455	141	283	366	372	328	357	316	382	378
Rb	86	115	97	25	48	73	103	41	45	35	70	28
Sr	269	115	132	35	129	34	173	152	131	282	233	262
Ba	280	236	161	222	78	118	217	125	122	42	105	210
Ga	20	21	29	17	25	18	19	18	24	35	34	24
Nb	19	19	35	8	50	28	33	32	16	37	45	56
Y	21	22	33	19	33	21	32	32	24	38	33	51
Zr	177	130	200	82	308	154	196	192	122	244	219	360

Table 1: (continuation)

Unit	LU	LU	LU	LU	LU	LU	LU	LU	LU	LU	LU	LU
Sample	B2-803	B2-804	B2-810	B2-811	B2-816	B2-828	B2-832	B2-833	B2-889	B2-907	B2-911	B2-913
Depth	1020 m	1022 m	1035 m	1036 m	1044 m	1062 m	1066 m	1067 m	1128 m	1150 m	1152 m	1153 m
SiO_2	55.59	50.07	49.95	49.84	43.65	50.06	47.87	50.43	48.98	49.74	47.45	48.78
TiO_2	1.40	2.10	3.83	0.86	3.62	2.94	2.68	2.72	2.11	2.82	3.07	3.75
Al_2O_3	18.15	14.78	14.16	10.55	10.68	11.14	14.43	14.68	15.44	17.37	16.24	14.27
$Fe_2O_3^{tot}$	8.27	11.69	14.21	12.25	14.74	13.22	12.03	12.59	12.99	11.75	12.24	13.75
MnO	0.06	0.15	0.19	0.18	0.15	0.17	0.16	0.19	0.21	0.19	0.22	0.27
MgO	4.49	8.44	4.73	12.87	8.03	9.62	6.66	6.74	7.38	3.64	5.25	5.28
CaO	3.89	7.55	8.31	10.04	14.10	9.08	8.12	8.27	9.02	10.87	11.23	10.08
Na_2O	3.20	0.68	1.31	0.83	0.89	0.88	2.23	2.27	1.39	0.99	1.09	1.94
K_2O	1.74	2.39	1.59	0.97	0.78	1.29	1.80	0.97	1.02	0.88	1.45	1.04
P_2O_5	0.18	0.24	0.76	0.10	0.75	0.39	0.37	0.40	0.28	0.48	0.69	0.21
LOI	3.05	2.26	1.25	1.86	2.27	1.65	3.45	1.07	1.62	1.29	1.33	0.77
Total	100.01	100.35	100.28	100.36	99.65	100.44	99.82	100.34	100.44	100.01	100.25	100.13
Cr	136	349	28	598	483	615	165	149	201	60	86	32
Ni	44	84	25	477	417	188	93	90	74	33	47	6
V	257	298	455	141	283	366	372	328	357	316	382	378
Rb	86	115	97	25	48	73	103	41	45	35	70	28
Sr	269	115	132	35	129	34	173	152	131	282	233	262
Ba	280	236	161	222	78	118	217	125	122	42	105	210
Ga	20	21	29	17	25	18	19	18	24	35	34	24
Nb	19	19	35	8	50	28	33	32	16	37	45	56
Y	21	22	33	19	33	21	32	32	24	38	33	51
Zr	177	130	200	82	308	154	196	192	122	244	219	360
Unit	LU	LU	LU									
Sample	B2-916	B2-917	B2-919	T-1/1	T-1/2	Gy-3/1	Gy-3/2	Gy-4	O-1	G-1		
Depth	1156 m	1157 m	1158 m									
SiO_2	47.74	46.49	47.38	50.57	46.47	48.39	46.61	50.34	47.65	49.93		
TiO_2	4.02	2.47	2.88	3.33	3.23	2.88	3.13	3.01	3.00	0.99		
Al_2O_3	14.48	15.14	15.06	15.14	14.57	13.98	14.23	14.42	14.45	18.37		
$Fe_2O_3^{tot}$	14.86	12.61	12.62	12.03	10.67	9.50	11.29	9.04	10.64	11.53		
MnO	0.22	0.18	0.20	0.16	0.21	0.21	0.26	0.16	0.18	0.18		
MgO	5.26	5.23	5.26	4.20	7.42	6.53	7.36	7.10	7.54	7.32		
CaO	8.94	12.68	10.95	10.14	10.97	9.42	10.35	9.45	10.40	11.44		
Na_2O	2.09	2.08	2.14	2.07	2.60	2.80	2.63	1.30	1.83	3.11		
K_2O	1.60	1.22	1.89	1.02	1.31	2.18	1.39	3.23	1.16	0.22		
P_2O_5	0.45	0.37	0.31	0.27	1.16	1.02	1.13	0.89	1.05	0.05		
LOI	0.79	1.77	1.58	2.36	2.87	1.53	2.13	2.11	2.40	2.07		
Total	100.44	100.24	100.26	101.29	101.48	98.44	100.51	101.05	100.30	105.21		
Cr	14	79	109	n.d.	n.d.	n.d.	n.d.	n.d.	n.d.	n.d.		
Ni	1	53	55	n.d.	n.d.	n.d.	n.d.	n.d.	n.d.	n.d.		
V	504	368	392	n.d.	n.d.	n.d.	n.d.	n.d.	n.d.	n.d.		
Rb	57	52	98	n.d.	n.d.	n.d.	n.d.	n.d.	n.d.	n.d.		
Sr	219	296	219	n.d.	n.d.	n.d.	n.d.	n.d.	n.d.	n.d.		
Ba	378	122	235	n.d.	n.d.	n.d.	n.d.	n.d.	n.d.	n.d.		
Ga	29	22	20	n.d.	n.d.	n.d.	n.d.	n.d.	n.d.	n.d.		
Nb	41	28	36	n.d.	n.d.	n.d.	n.d.	n.d.	n.d.	n.d.		
Y	32	30	28	n.d.	n.d.	n.d.	n.d.	n.d.	n.d.	n.d.		
Zr	204	175	204	n.d.	n.d.	n.d.	n.d.	n.d.	n.d.	n.d.		

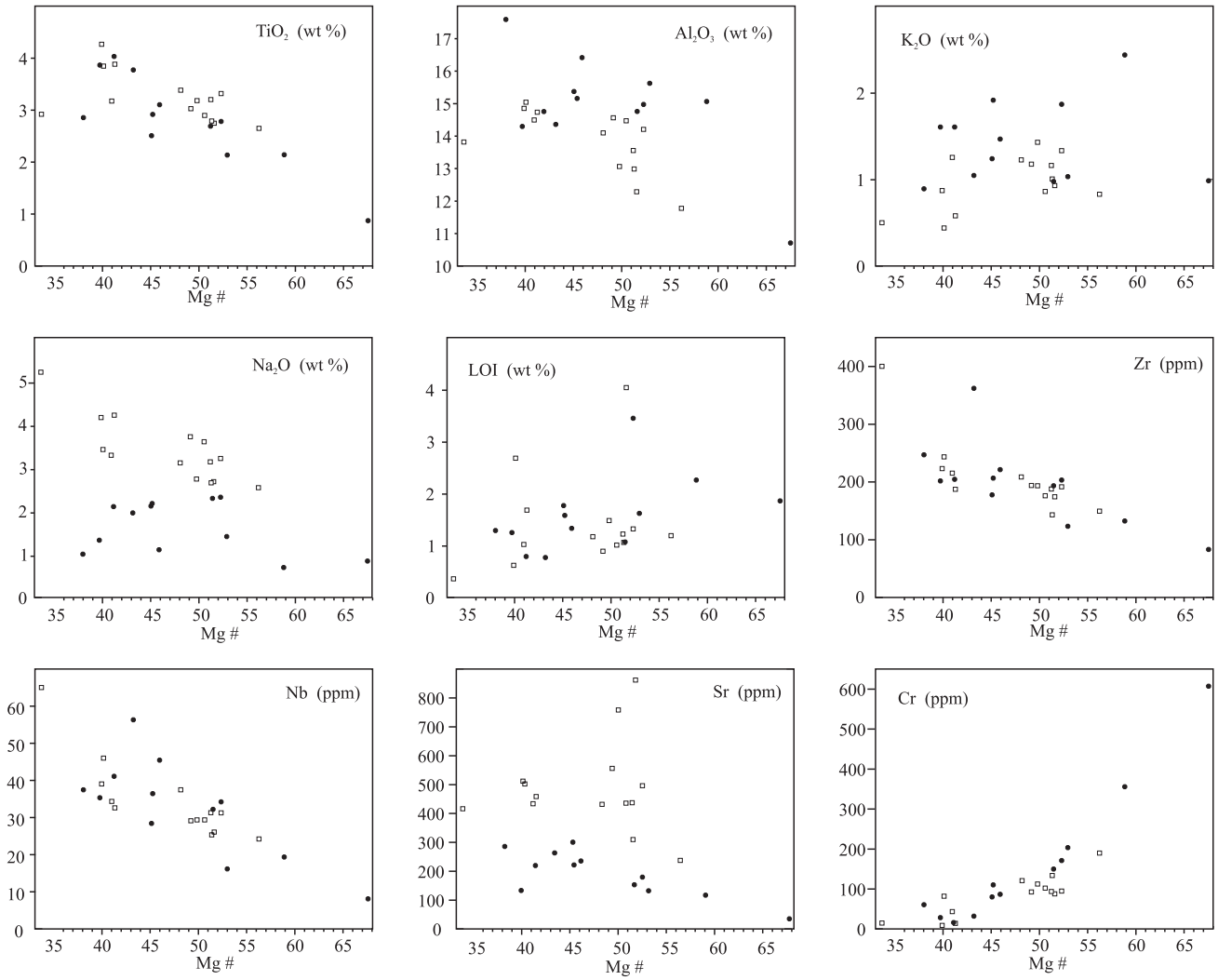

Figure 5: Harker diagrams with Mg# as a differentiation index. Symbols as in Fig. 4.

usually used for sketching the characteristics of the ancient igneous rocks. The major and trace element compositions of UU and LU amphibolites are evaluated below.

4.2.1. Major elements

The two petrographically different units show clear differences in their major element compositions (Table 1). On the TAS diagram (LE MAITRE, 1989, Fig. 4), rock samples of UU are plotted close to the alkali basalt field, while those belonging to LU are more differentiated and are subalkali in character (Fig. 4 inset, IRVINE & BARAGAR, 1971). Using either Zr or Mg# (Mg/(Mg+Fe)) as a differentiation index, the two sample groups exhibit different evolution trends for most elements on the series of Harker diagrams (Fig. 5). There are only a few outliers, probably affected by post-magmatic alteration processes. Generally, the UU samples are characterized by lower Si, K, and Al and higher Fe, Ti, and Na than those of the LU (Table 1).

Co-variation of LOI and Mg# in both units suggests that, mainly because of the presence of amphibole and chlorite, samples with the most primitive composition are the most hydrated. For this reason, LOI is insensitive to the effects of any post-magmatic processes and so the commonly used bivariate correlation between LOI and Na_2O is not a suitable tool to test the origin of extra Na in the UU. Nevertheless, the low values (–0.14 for the UU, 0.10 for the LU) of the partial correlation coefficient between LOI and Na_2O (controlling for Mg#) suggest that Na-concentration is independent of LOI, and so the different Na-content of the two units is probably a primary igneous feature. (The partial correlation coefficient is the correlation that remains between two variables after removing the relationship that is due to their mutual association with a third variable.) The same is true for K_2O and Al_2O_3, which exhibit even lower values than Na_2O in the analogous calculation for both units. Weathering trends using major element diagrams of NESBITT & YOUNG (1989) indicate only a slight decrease in FeO+MgO relative to the average basalt composition. Nevertheless, in good agreement with the low partial correlation coefficients, no remarkable increase in either Na_2O or K_2O is suggested. Moreover, there is no difference in the weathering trends of the two groups on any of these plots, confirming that post-magmatic processes have only a subordinate role in the above chemical differences.

The agpaitic coefficient ($(Na_2O+K_2O)/Al_2O_3$, molar proportions) in the UU is in the range typical for alkali basalts, varying between 0.43 and 0.52. For the LU, the agpaitic index varies around 0.21 for both the most and the least differentiated samples. Even UU samples are, on the other hand, free of normative nepheline or acmite. Mg# is below 60 for all but one sample and is therefore differentiated. Some samples are even highly differentiated (Mg# < 45).

4.2.2. Trace elements

The strong negative correlation between Mg# and Zr (–0.72) suggests that both variables are good indicators of igneous differentiation (Fig. 5). Ga, Zr, Nb, and Y, elements which are usually immobile during the post-magmatic processes (e.g. WOOD et al., 1976; COISH, 1977; MORRISOn, 1978) increase with ongoing differentiation in both units, thus indicating incompatibility. Cr and Ni decrease during the fractionation, while the third transition metal (V) is slightly incompatible, similar to Fe and Mn. K, Rb, Ba, and Nb slightly scatter in LU, while they exhibit a clear increasing trend in the case of the UU. Sr shows a pattern similar to that of Na_2O. It is incompatible in both units, with remarkably, the highest concentrations in the UU.

Although N-MORB normalized values for the two rock units show similar ranges for most elements, the typical spectra differ more in detail (Table 2, Figs. 6a and 6b). K, Ba, and Rb show significant gains in both cases, having larger concentrations in the LU. Nb-enrichment up to 10*N-MORB is typical for both sample groups. The UU samples are significantly higher in Sr and Ti than the LU ones. In the case of these two elements the LU is close to MORB composition with element/MORB ratios as low as 1–2. This also is typical for the Y-content of both groups. UU samples are rather low in transition metals and exhibit a spectrum from the heaviest to the lightest elements with an approximately continuous slope, suggesting a pattern of pure igneous origin. Also the very narrow range of element ratios, like Rb/Nb (0.5–1.5) and K_2O/Nb (0.02–0.05), argues against any significant effect of post-magmatic enrichment processes. LU samples are similarly low in all elements relative to N-MORB up to Sr, while they show an abrupt enrichment for K, Rb, Ba, and Nb, exhibiting a trend which suggests an average net gain. Multi-element variation patterns in good agreement with the major elements show that UU samples are alkali basalts without any significant change of the original igneous composition. The LU elements, in contrast, represent subalkali basalts and basaltic andesites with enrichment of Nb, K, Rb, and Ba, probably caused either by K-metasomatism or by assimilation of the upper continental crust or pelagic sediments (FLOYD et al., 1996). The positive Nb anomaly, nevertheless, shows that assimilation of the lower crust is unlikely (THOMPSON et al., 1982).

4.3. Mineral chemistry

A few amphibole and plagioclase compositions from both the upper and the lower amphibolites were presented previously by ÁRKAI et al. (1999) and used for thermobarometric calculations. In both units, amphibole exhibits a common hornblende composition, while matrix plagioclase varies around An_{33}. As these results are confirmed by the new measurements, only the compositions of relict phases from the LU are given below (Table 3.). Garnet is not zoned; different grains in different samples have a constant composition

Table 2: Average N-MORB normalized compositions of the two units. N-MORB composition is after SUN & MCDONOUGH (1989).

Element	Upper Unit/ N-MORB	Lower Unit/ N-MORB
Cr	0.25±0.15	0.60±0.60
Ni	0.36±0.20	0.75±0.96
Y	0.91±0.26	0.83±0.23
Ti	1.97±0.29	1.70±0.55
Zr	1.96±0.60	1.90±0.67
Sr	4.26±1.35	1.58±0.74
Nb	8.85±1.72	9.70±3.20
K	8.33±2.69	11.95±3.96
Ba	11.9±4.20	12.7±6.33
Rb	32.0±22	51.48±23

Table 3: Representative mineral compositions of relict phases from the LU amphibolites.

	Grt	Pl inclusion in Grt	Ilm inclusion in Grt	Bt in Bt-Qz symplectite	Amp	Pl inclusion in Amp
SiO_2	38.18	54.80	0.00	39.22	43.11	46.94
TiO_2	0.18	0.00	51.35	2.66	0.48	0.00
Al_2O_3	21.37	29.12	0.59	15.55	11.32	30.37
FeO	29.16	0.16	47.05	16.49	16.47	1.18
MnO	0.72	0.05	2.07	0.06	0.26	0.00
MgO	2.80	0.00	0.05	14.94	9.17	0.54
CaO	7.87	9.93	0.12	0.00	10.49	19.20
Na_2O	0.00	4.60	0.00	0.00	0.90	0.74
K_2O	0.01	0.10	0.00	8.98	0.44	0.07
Total	100.34	98.77	101.23	98.11	92.69	99.04
No. O	12	8	3	22	24	8
Si	3.01	2.48	0.00	5.69	7.04	2.20
Ti	0.01	0.00	0.97	0.30	0.06	0.00
Al	1.99	1.56	0.02	2.66	2.18	1.68
Fe	1.92	0.01	0.99	2.00	2.25	0.05
Mn	0.05	0.00	0.04	0.01	0.04	0.00
Mg	0.33	0.00	0.00	3.23	2.23	0.04
Ca	0.67	0.48	0.00	0.00	1.83	0.96
Na	0.00	0.40	0.00	0.00	0.28	0.07
K	0.00	0.01	0.00	1.66	0.09	0.00
No. cation	7.98	4.94	2.02	15.54	16.00	5.00

of $Alm_{61-63}Sps_{1-2}Prp_{10-12}Grs_{22-25}$. Mn in ilmenite, surrounding rutile inclusions is as low as 0.04 p.f.u. Symplectitic biotite is magnesian, having Mg/(Mg+Fe) ~ 0.66 with Ti ~ 0.33 and Si ~ 6.00. The biotite of the matrix is much lower in Ti, varying around 0.15 p.f.u. Plagioclase in the Qz-Pl symplectite is ~ An_{90} both as amphibole inclusions and as a matrix constituent. Plagioclase intergrown with biotite and quartz in the other symplectite type is a little more sodic, being $An_{82}Ab_{15}Or_3$. For feldspar grains in the rutile-ilmenite-plagioclase inclusion assemblage in garnet (GRIPS), An_{55} is typical. All these feldspar compositions differ significantly from those that characterize the matrix and represent the conditions of the amphibolite facies overprint.

5. DISCUSSION AND CONCLUSIONS

5.1. LU and UU discrimination

5.1.1. Palaeotectonic setting of amphibolite formation

The amphibolite samples of the Baksa-2 borehole exhibit different chemical compositions as well as fractionation histories in the upper and the lower segments of the rock column. Whether or not they formed in different palaeotectonic situations can be tested by a series of discrimination diagrams. Several of these approaches (Zr-Ti-Y, PEARCE & CANN, 1973, Fig. 6c; Zr-Nb-Y, MESCHEDE, 1986; Zr-Zr/Y, PEARCE & NORRY, 1979, Fig. 6d; Ti/Y-Zr/Y, PEARCE & GALE, 1977; Th-Zr-Nb, WOOD, 1979) give identical results; both the UU and the LU samples represent WP basalts. However, the two groups of samples define different clouds and trends on most of these plots due to the aforementioned differences in Ti, Zr, and Nb. On the Zr-Zr/Y plot, the UU samples define quite a flat trend, corresponding to an Ol+Cpx+Pl-dominated fractional crystallization of an enriched mantle source.

In contrast, LU samples define a steep line, suggesting a slight depletion relative to the primitive mantle (Fig. 6d). This trend may be caused by fractional crystallization in which garnet is also involved. This also seems to be confirmed by the rapid decrease of Cr along the differentiation path (from 607 down to 32 ppm), while Zr increases from 83 to 362 ppm (PEARCE and NORRY, 1979). The incompatible behaviour of Ga, however, disproves this idea as $K_{d,Ga}^{gar/melt} > 10$. The rapid decrease of Y shown in Fig. 6d may be the result of amphibole crystallization as is also suggested by the flat curve of the V (Zr:123 → 362 ppm; V: 361 → 380 ppm).

Considering all the diagrams discussed above, it is concluded that UU samples represent WP alkali basalt, while samples belonging to the LU are more differentiated WP andesites and basalts, which probably assimilated pelagic sediments.

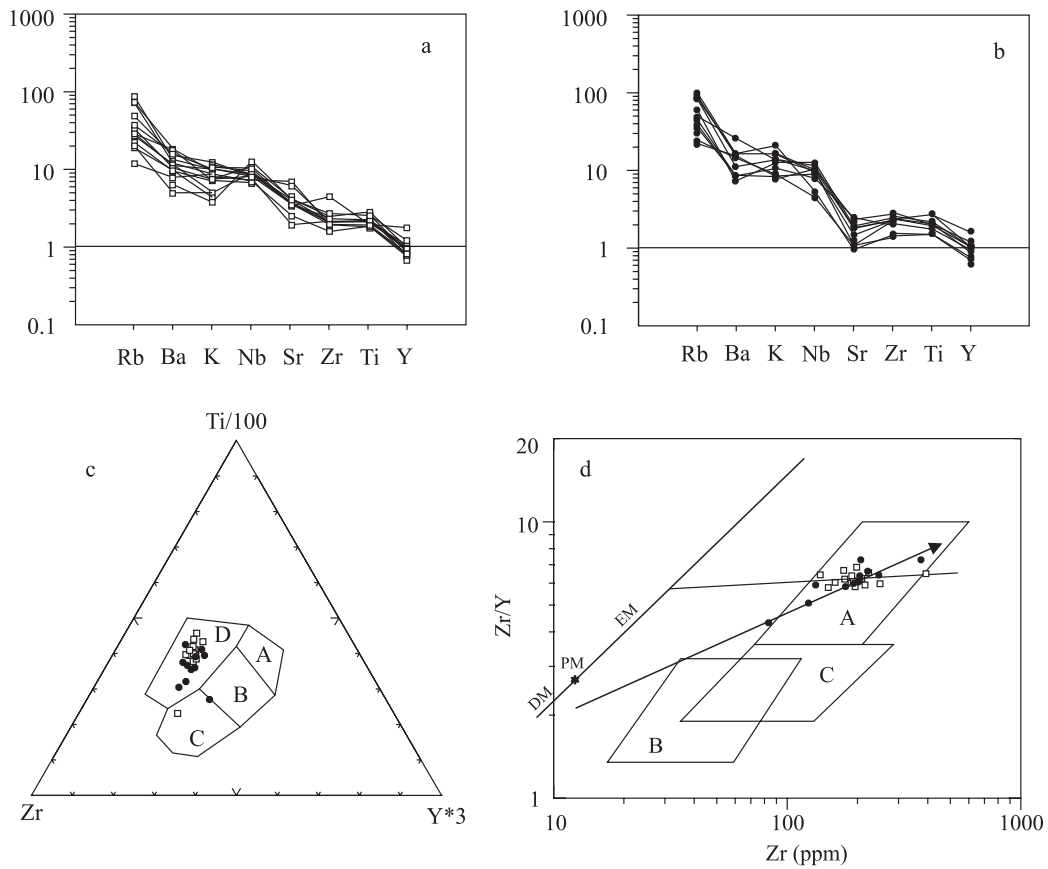

Figure 6: Geochemical data of the present study plotted on N-MORB normalized spidergrams for a) UU and b) LU samples. Data plotted on the c) Zr-Ti-Y diagram (PEARCE & CANN, 1973) (A, B: low-K tholeiites; B, C: calc-alkaline basalts; B: ocean floor basalts; D: within-plate basalts), d) Zr-Zr/Y diagram (PEARCE & NORRY, 1979) (A: within-plate basalts; B: island arc basalts; C: mid-ocean ridge basalts; PM: primitive mantle; DM: depleted mantle; EM: enriched mantle). Symbols as in Fig. 4.

An alternative model would be the assumption of a similar alkali basalt protolith for both UU and LU. In this scenario the striking difference found in the chemical compositions would be the result of different post-magmatic alteration histories which caused net gains in K, Rb, Ba, and Nb in the LU and relative increases in Na and Sr in the case of the UU. The total independence of the mobile components of LOI, as well as clear co-variation of all these elements with Zr, nevertheless, makes this model improbable.

5.1.2. Discriminant function analysis

The mineralogy and the major and trace element geochemistry shows that amphibolites of the Baksa-2 well can clearly be divided into two distinct groups. Whether the difference between the chemical compositions of the two sample groups is statistically significant or not can be checked using the independent samples t-test. Comparing LU and UU samples element by element, at a significance level of 95% the difference becomes significant with regard to SiO_2, TiO_2, Na_2O, K_2O, Cr, Sr, and Rb. An initial attempt is made here to extend this division to all samples taken from the literature (SZEDERKÉNYI, 1983, and references therein) in order to be able to define subareas of the Görcsöny Ridge. Discriminant function analysis (e.g. RAGLAND et al., 1997, and references therein) based on the whole data set was applied for this purpose. This approach is suitable for calculating the optimal function of variables (the discriminant function), for distinguishing between two (or more) known sample groups (UU and LU amphibolites in the present case). In the calculations a stepwise method with Wilks' lambda minimization was used. It was found that the best function discriminating the two units is:

$$D1 = 1.3\ MgO + 1.1\ Na_2O + 0.5\ TiO_2 + 0.9\ Sr.$$

Using this linear combination of elements, the two groups can be clearly distinguished from each other (Fig. 7a). This function confirms the previous observations that the UU samples are alkali basalts and hence are significantly higher in Mg, Na, Ti, and Sr than those of the LU. As there is a strong negative correlation between Al and Mg (r = –0.72), Al does not appear in the above function. Using only major elements for discriminating historical samples taken from the literature, the function has the form of

$$D2 = 1.2\ Na_2O - 0.6\ Al_2O_3 - 0.5\ SiO_2.$$

On the appropriate $Na_2O - (Al_2O_3+SiO_2)$ plot (Fig. 7b), samples of the boreholes T-1 (one of the two), Ok-1, and Gy-4 undoubtedly belong to the LU, while the second sample of T-1, the G-1 eclogite, and both Gy-3 samples lie at the border between LU and UU. Each Baksa-2 sample taken from the previous literature is plotted in the appropriate group defined by the whole database.

5.1.3. Petrological modelling of the magmatic rock compositions

Although UU samples contain no normative nepheline, the other geochemical features discussed above undoubtedly prove that they represent alkali basalts. An independent way of performing CIPW norm calculations is to reconstruct the primary mineral composition of the protolith by using thermodynamic calculations at the *P-T* conditions of crystallization. The DOMINO/THERIAK code of DE CAPITANI (1994) is applied, which uses Gibbs free energy minimization to compute the complete, stable assemblage at each *P-T* point. DOMINO is particularly useful for analyzing relict parageneses because it computes the complete, stable assemblage at each stage of a given *P-T* evolution. Provided the bulk composition of a rock is adequately estimated and the thermodynamic properties of all phases involved are sufficiently well known, then the computed phase diagram may be directly compared to the observed assemblages. Given that each phase diagram is computed for a fixed bulk composition, the model must be sufficiently close to reality to represent all of the phases observed. The thermodynamic database used here is an extended version of BERMAN (1988) with modifications from MEYRE et al. (1997).

Assuming a wide *P-T* window and constant fluid composition (*T*: 800–1300 °C, *P*: 3–8 kbar, $FeO/(FeO+Fe_2O_3)$ = 0.9, excess H_2O) for the crystallization condition, LU samples contain Ol, Amp, Cpx, Pl, Mag, Kfs, Bt, Ilm, and Qz ±

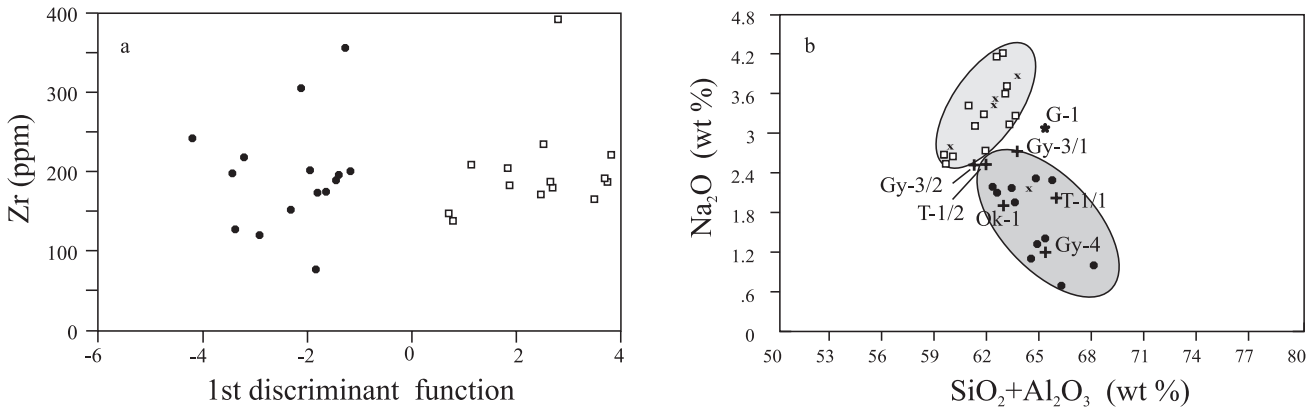

Figure 7: a) Plot of scores of the D1 discriminant function versus Zr. b) Na_2O-$(Al_2O_3+SiO_2)$ plot for all Görcsöny Ridge amphibolites. Borehole abbreviations are given in Fig. 2. Symbols as in Fig. 4.; "+" denotes other wells; "x" stands for previous data for Baksa-2 (SZEDERKÉNYI, 1983).

Table 4: Model mineral compositions for UU and LU amphibolites under crystallization conditions. Because of the significant bias from a normal distribution, the median and interquartile range (IQR) are used to characterize the data sets.

Phases	UU				LU			
	Median	IQR	Min	Max	Median	IQR	Min	Max
Cpx	27.0	7.9	4.5	49.1	13.4	9.3	4.0	39.0
Ol	16.7	7.1	4.3	22.3	17.6	8.6	9.7	22.9
Pl	40.2	8.1	21.9	53.8	30.1	8.1	17.8	41.1
Kfs	4.8	1.9	2.1	18.6	4.9	2.8	3.1	9.4
Qz	0	0	0	2.7	25.7	17.6	0.5	41.4
Nph	1.8	4.7	0	11.3	0	0	0	0
Mag	2.1	0.3	1.3	4.1	2.0	1.9	0.7	4.5
Ilm	9.0	1.5	3.5	12.2	7.1	2.4	1.9	10.3

Opx in different proportions (mineral abbreviations after WHITNEY & EVANS, 2010). Amphibole and biotite are missing above 900 °C. UU samples do not contain Qz, and all but a few of them contain a significant amount of nepheline (up to 12 v/v%) in addition to the above phases. The amounts of Pl (> 40 v/v%) as well as Cpx (> 25 v/v%) significantly exceed the typical values of the LU (< 30 v/v% for Pl, < 15 v/v% for Cpx). The average modelled mineral compositions for both units are given as median values, interquartile ranges, and minimum and maximum values in Table 4. Given the significant bias from a normal distribution, mean and standard deviation values are not informative. Gy-3, G-1, and T-1 samples, which are plotted at the border between UU and LU samples in Fig. 7b, contain no nepheline based on the present calculation and are therefore more similar to LU.

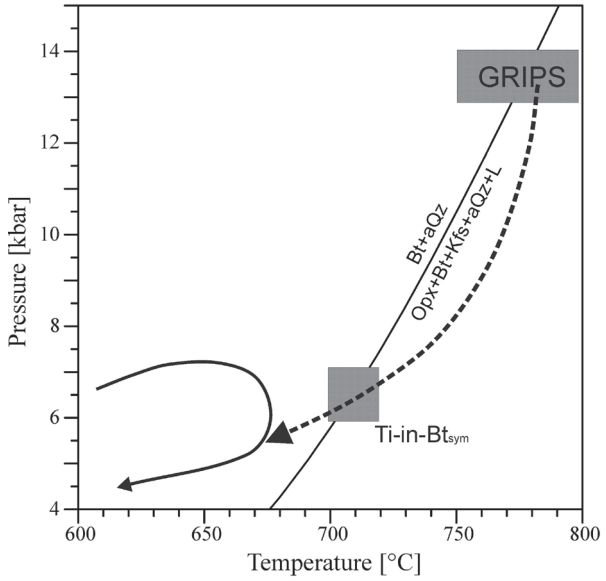

Figure 8: Summary of the thermobarometric data for the Görcsöny Complex. The solid line represents the results of previous calculations (KIRÁLY, 1996; ÁRKAI et al., 1999) for LU and UU samples, while the dashed line stands for the early evolution of LU amphibolites. Ti-in-Bt temperatures were calculated using HENRY et al. (2005); for GRIPS paragenesis the barometer of BOHLEN & LIOTTA (1986) was used. The Opx breakdown reaction was computed with DOMINO/THERIAK (DE CAPITANI, 1994) using the composition of symplectite biotite.

All things considered, the two exclusive model assemblages define quartz andesite (LU) and nepheline basalt or tephrite (UU) as the most likely protoliths. The two amphibolite types therefore represent different kinds of primary magmas and significantly different fractionation histories.

5.1.4. Basic consequences for mineralogical composition

The question of whether the above chemical differences can explain the observed differences in the mineral composition between UU and LU amphibolites should still be answered. The most striking difference is that UU rocks are free of Rt, Bt, and Grt; moreover LU samples exhibit a wide spectrum of textural relics. Garnet in the LU amphibolite cannot be an igneous relic phase because of the incompatible behaviour of Ga (see above), and therefore must be metamorphic in origin. Rutile, under identical physical conditions, can replace ilmenite in Mg-rich rocks (RAASE, 1974); here however, Rt appears exclusively in the LU samples which are lower in Mg. So the stability field of this Ti-phase must have been determined by a somewhat different *P-T* evolution for the LU samples. Based on their common co-existence, the pre-kinematic, Grt- and Rt-bearing paragenesis suggests an early higher pressure event for the LU section. Although its amount is also hard to quantify, radial cracks around faceted plagioclase inclusions in garnet imply significant decompression (VAN DER MOLEN &VAN ROERMUND, 1986) and thus suggest higher pressure metamorphism, too.

As only a few garnet, plagioclase, and biotite grains with original composition have been preserved in the samples, there is only a very limited possibility to reconstruct the physical conditions of this early event. Based on a DOMINO/THERIAK model using the measured biotite composition, the fine-grained Bt+Qz+Kfs symplectite preserved suggests the presence of a previous orthopyroxene. The appearance of similar symplectites in mafic granulites was reported by OGILVIE et al. (2004), BARBOSA et al. (2006), and DOS SANTOS et al. (2011), among several others, who explain Opx breakdown due to the Opx+Kfs+liquid = Bt+Qz reaction, which is the same as the result of our model (Fig. 8). Others found this symplectite evidence for retrograde breakdown of garnet (PRAKASH et al., 2012; GRANTHAM et al., 2013) or K-feldspar (WATERS, 2001; SAJEEV & OSANAI, 2004). There is, however no textural indication of garnet decomposition in the studied amphibolite samples.

Biotite has different compositions in diverse textural positions. Matrix biotite is relatively low in Ti and suggests a formation temperature of ~ 580 °C (Fig. 9, HENRY et al., 2005) in accordance with the conditions previously calculated for the second metamorphic event. The fact that the Ti-content of Bt in Opx replacing symplectite is twice as high, however, implies a formation temperature of 700–720 °C using the same approach (Fig. 9). Together with the above calculation, biotite appears around 710 °C at 7 kbar along a retrograde pathway. In a wide temperature range of 750–800 °C, the GRIPS barometer (BOHLEN and LIOTTA, 1986)

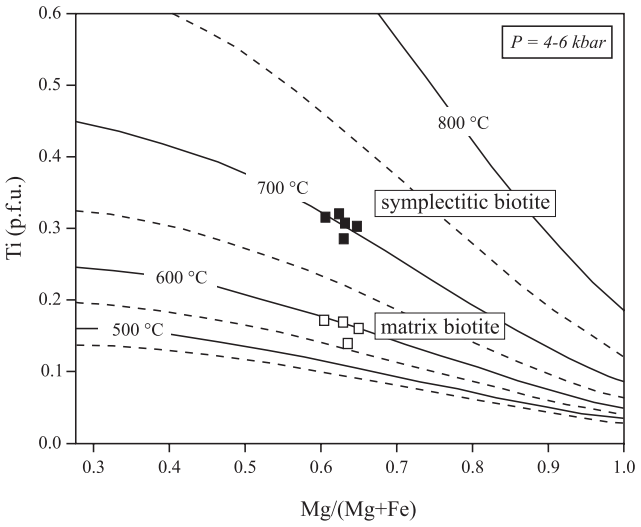

Figure 9: Ti-in-biotite thermometric plots (HENRY et al., 2005) for Bt+Qz+Kfs symplectite and matrix biotite.

shows 13–14 kbar for the Rt+Pl+Ilm inclusion paragenesis in garnets of the LU amphibolites for five independent cases (Fig. 8). Although the presence of calcic myrmekite suggests HT metamorphic conditions (EFIMOV et al., 2010), it is not suitable for estimating *P-T* conditions quantitatively.

Although there are only a few, uncertain thermobarometric data, the conflicting metamorphic evolutions for the LU and UU segments are proven, and an early HP metamorphic event followed by close to isothermal decompression for the LU amphibolites can be supposed.

5.1.5. Geodynamic consequences

In an opening continental rift region, igneous rocks of different compositions may form simultaneously, resulting in a significant overlap in both space and time. In the case of the Görcsöny Ridge, however, the diverse rock types occur separately, suggesting that the two segments may represent different realms of the same ocean. UU samples may have formed in the early phase of continental rifting and therefore represent a typical marginal sea, which is also confirmed by their metasedimentary rock surroundings (carbonates, graphite schist). LU, on the other hand, represents a sea mountain on a prior oceanic floor. The within plate geochemical character, (the trace element pattern that shows enrichment with respect to N-MORB) is compatible with OIB (ocean island basalt) origin.

Additionally, the appearance of ultramafic bodies in the Görcsöny Complex as well as the numerous reports of eclogite occurrences suggests that rocks of the Görcsöny Complex likely represent different segments of a juxtaposed consuming ocean, supporting a tentative threefold scenario sketched in Fig. 10a–c.

1) The protoliths of the LU and UU amphibolites developed in various palaeotectonic settings (Fig. 10a), resulting in different chemical compositions.
2) A subduction-related metamorphic evolution led to HP metamorphism of the LU, while the UU was affected exclusively by an MP event (Fig. 10b).
3) Probably due to reversal of the transport direction from subduction to uplift of the LU slice (e.g. following the model of CHEMENDA et al., 1995), the two units became juxtaposed and exhibit identical metamorphic evolutions from this point on (Fig. 10c).

Samples with geochemical characteristics similar to those of the UU of the Baksa-2 well do not occur in the other wells studied, where LU rocks form the top of the basement. The spatial distribution of these wells (Fig. 2) makes the spatial extension of the two distinct units approximately possible even in the absence of available petrological data in older wells. It is, nevertheless, worth mentioning that all known serpentinite bodies, eclogite, and garnetiferous amphibolite localities appear in the territory of the assumed extended realm of the LU, north of the Baksa-2 well (Fig. 10d). Thermobarometric data calculated for LU amphibolites are consistent with the *P-T* evolution suggested by the relict assemblages of the host garnetiferous gneiss samples (NAGY &

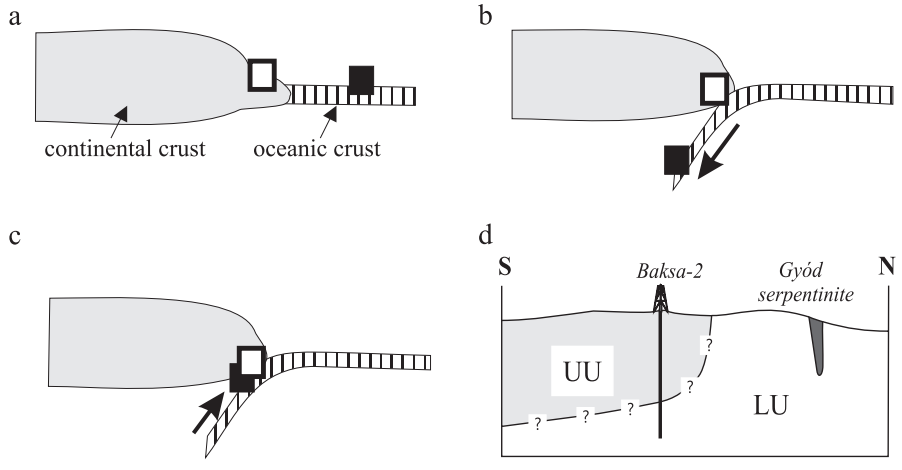

Figure 10: a–c) A tentative threefold scheme for the geodynamic evolution of the Görcsöny Ridge (white square: UU; black square: LU). (d) Theoretical N–S section across the Görcsöny Complex. For details see text.

TÓTH, 2009), implying that the early metamorphic phase can be extended for the whole lower segment of the Baksa-2 well. Furthermore, the results of the geochemical classification of the amphibolites suggest that this evolution may also be typical for a significant part of the Görcsöny Ridge.

Although the pre-metamorphic and early metamorphic histories of the two regimes differ significantly, the peak conditions of the last Barrovian metamorphism in the two slices are identical (ÁRKAI et al., 1999). As the amphibole and biotite cooling ages are also the same in the two units (LELKES-FELVÁRI & FRANK, 2006), they probably became juxtaposed during the Variscan orogeny and suffered the common retrograde evolution after nappe formation.

This tectonometamorphic scheme is compatible with the slab break-off model developed by von BLANCKENBURG & DAVIES (1995) for the Alpine evolution of the Central Alps. This process, nevertheless, was also found to be important for the exhumation of HP metamorphic rocks throughout the Variscan orogeny (O'BRIEN, 2000). Published *P-T* paths for the HP granulites of the Bohemian Massif are rather similar to those reconstructed for LU rocks; these pathways are in general dominated by initial near-to-isothermal decompression followed by a near-to-isobaric cooling stage (KOTKOVÁ, 2007). The resulting collisional orogen exhibits a rather complex structure in which the amalgamated continental and oceanic fragments are juxtaposed, being separated in large scale nappe systems (e.g. MATTE et al., 1990; OLIVER et al., 1993). The contrasting geochemical characters as well as metamorphic histories of the UU and LU blocks together with numerous previous results suggest that the Görcsöny Ridge is a tectonic assemblage of blocks of different metamorphic evolutions.

Blocks with different metamorphic evolutions were also inferred in the Slavonian Mountains, where, in addition to the common medium pressure varieties, amphibolites and host metapelitic rocks with peak conditions of 600–660 °C and 11–12 kbar also occur (BALEN et al., 2006; HORVÁTH et al., 2010). These observations further strengthen the genetic relationship between the two neighbouring areas inside the SW Tisza. Nevertheless, in order to specify similarities and differences between their evolution more accurately, further petrological studies must be performed.

ACKNOWLEDGEMENT

The project was financially supported by the OTKA foundation (grant No. F 017366).

REFERENCES

ÁRKAI, P. (1984): Polymetamorphism of the crystalline basement of the Somogy-Dráva Basin (Southwestern Transdanubia, Hungary).– Acta Mineralogica-Petrographica, Szeged XXVI, 129–153.

ÁRKAI, P., NAGY, G. & DOBOSI, G. (1985): Polymetamorphic evolution of the South Hungarian crystalline basement, Pannonian Basin: geothermometric and geobarometric data.– Acta Geologica Hungarica, 28, 165–190.

ÁRKAI, P., HORVÁTH, P. & NAGY, G. (1999): A clockwise P-T path from the Variscan Basement of the Tisza Unit, Pannonian Basin, Hungary.– Geologica Croatia, 52/2, 109–117.

ÁRKAI, P. & NAGY, G. (1994): Tectonic and magmatic effects on amphibole chemistry in mylonitized amphibolites and amphibole-bearing enclaves associated with granitoid rocks, Mecsek Mountains, Hungary.– Acta Geologica Hungarica, 37/3–4, 235–268.

BALEN, D., HORVÁTH, P., TOMLJENOVIC, B., FINGER, F., HUMER, B., PAMIĆ, J. & ÁRKAI, P. (2006): A record of pre-Variscan Barrovian regional metamorphism in the eastern part of the Slavonian Mountains (NE Croatia).– Mineralogy and Petrology, 87, 143–162.

BALLA, Z. (1983): A dél-dunántúli ultrabázitok lemeztektonikai értelmezése. (Plate tectonic interpretation of ultrabasites in Southern Transdanubia. in Hungarian).– Földtani Közlöny, 113, 39–56.

BALLA, Z. & GYALOG, L. (eds.) (2009): Geology of the North-eastern Part of the Mórágy Block: Explanatory Notes to the Geological Map-series of the North-eastern Part of the Mórágy Block (1:10 000).– MÁFI, Budapest,. 283 p.

BARBOSA, J., NICOLLET, C., LEITE, C., KIENAST, J.R., FUCK, R.A. & MACEDO, E.P. (2006): Hercynite–quartz-bearing granulites from Brejões Domearea, Jequié Block, Bahia, Brazil: Influence of charnockite intrusion on granulite facies metamorphism.– Lithos, 92, 537–556.

BERMAN, R.G. (1988): Internally-consistent thermodynamic database for stoichiometric minerals in the system Na_2O-K_2O-CaO-MgO-FeO-Fe_2O_3-Al_2O_3-SiO_2-TiO_2-H_2O-CO_2.– Journal of Petrology, 29, 445–522.

BOHLEN, S.R. & LIOTTA, J.J. (1986): A barometer for garnet amphibolites and garnet granulites.– Journal of Petrology, 27, 1025–1034.

BUDA, GY. (1981): Genesis of the Hungarian granitoid rocks.– Acta Geologica Hungarica, 24, 309–318.

CHEMENDA, A.I., MATTAUER, M., MALAVIEILLE, J. & BOKUN, A.N. (1995): A mechanism for syn-collisional rock exhumation and associated normal faulting: Results from physical modelling.– Earth and Planetary Science Letters, 132, 225–232.

COISH, R.A. (1977): Ocean Floor metamorphism in the Betts Cove ophiolite, Newfoundland.– Contributions to Mineralogy and Petrology, 60, 255–270.

CSONTOS, L., NAGYMAROSI, A., HORVÁTH, F. & KOVAĆ, M. (1992): Tertiary evolution of the Intra-Carpathian area: a model.– Tectonophysics, 208, 221–241.

DE CAPITANI, C. (1994): Gleichgewichts-Phasendiagramme: Theorie und Software.– Beihefte zum European Journal of Mineralogy, 72. Jahrestagung der Deutschen Mineralogischen Gesellschaft, 6, 48.

DOS SANTOS, T.M.B., MUNHÁ, J.M., TASSINARI, C.C.G. & FONSECA, P.E. (2011): The link between partial melting, granitization and granulite development in central Ribeira Fold Belt, SE Brazil: New evidence from elemental and Sr eNd isotopic geochemistry. – Journal of South American Earth Sciences, 31, 262–278.

DYMEK, R.F. & SCHIFFRIES, C.M. (1987): Calcic myrmekite: possible evidence for the involvement ofwater during the evolution of andesine anorthosite from St-Urbain, Quebec.– Canadian Mineralogist, 25, 291–319.

EFIMOV, A.A., FLEROVA, K.V. & MAEGOV, V.I. (2010): The first find of calcic myrmekite (quartz-plagioclase symplectites) in Uralian gabbro.– Geochemistry, 435/1, 1450–1455.

FINTOR, K., SCHUBERT, F. & TÓTH T.M. (2008): Hiperszalin paleofluidum-áramlás nyomai a Baksai Komplexum repedésrendszerében. (Indication of hypersaline palaeofluid migration in the fracture system of the Baksa Complex. in Hungarian).– Földtani Közlöny, 138/3, 257–278.

FINTOR, K., TÓTH T.M. & SCHUBERT, F. (2009): A Baksai Komplexum posztmetamorf fluidum evolúciója. (Post-metamorphic fluid

evolution of the Baksa Complex in Hungarian).– In: TÓTH, T.M. (ed.): Magmás és metamorf képződmények a Tiszai Egységben. GeoLitera, 245–258.

FINTOR, K., TÓTH T.M. & SCHUBERT, F. (2010): Near vein metasomatism along propylitic veins in the Baksa Gneiss Complex, Pannonian Basin, Hungary.– Geologia Croatica, 63/1, 75–91.

FINTOR, K., TÓTH T.M. & SCHUBERT, F. (2011): Hydrothermal palaeofluid circulation in the fracture network of the Baksa Gneiss Complex of SW Pannonian Basin, Hungary.– Geofluids, 11/2, 144–165.

FLOYD, P.A., WINCHESTER, J.A., CIESIELCZUK, J., LEWANDOWSKA, A., SZCZEPANSKI, J. & TURNIAK, K. (1996): Geochemistry of early Paleozoic amphibolites from the Orlica-Śnieżnik dome, Bohemian massif: petrogenesis and palaeotectonic aspects.– Geologische Rundschau, 85, 225–238.

FÜLÖP, J. (1994): Magyarország geológiája. Paleozoikum II. (Geology of Hungary. Paleozoic II. In Hungarian).– Akadémiai kiadó, 447 p.

GRANTHAM, G.H., MACEY, P.H., HORIE, K., KAWAKAMI, T., ISHIKAWA, M., SATISH-KUMAR, M., TSUCHIYA, N., GRASER, P. & AZEVEDO, S. (2013): Comparison of the metamorphic history of the Monapo Complex, northern Mozambique and Balchenfjella and Austhameren areas, Sør Rondane, Antarctica: Implications for the Kuunga Orogeny and the amalgamation of N and S. Gondwana.– Precambrian Research, 234, 85–135.

HAAS, J., KOVÁCS, S., KRYSTYN, L. & LEIN, R. (1995): Significance of Late Permian-Triassic facies zones in terrane reconstructions in the Alpine-North Pannonian domain.– Tectonophysics, 242, 19–40.

HENRY, D.J., GUIDOTTI, C.V. & THOMSON, J.A. (2005): The Ti-saturation surface for low-to-medium pressure metapelitic biotite: Implications for Geothermometry and Ti-substitution Mechanisms.– American Mineralogist, 90, 316–328.

HORVÁTH, P., KOVÁCS, G. & SZAKMÁNY, GY. (2003): Eclogite and garnetiferous amphibolite gravels from Miocene conglomerates: new results for the Variscan metamorphic evolution of the Tisza Unit (Pannonian Basin, Hungary).– Geologica Carpathica, 54/6, 1–12.

HORVÁTH, P., BALEN, D., FINGER, F., TOMLJENOVIĆ, B. & KRENN, E. (2010): Contrasting P-T-t paths from the basement of the Tisia Unit (Slavonian Mts., NE Croatia): Application of quantitative phase diagrams and monazite age dating.– Lithos, 117, 269–282.

IRVINE, T.N. & BARAGAR, W.A.R. (1971): A guide to the chemical classification of the common volcanic rocks.– Canadian Journal of Earth Sciences, 8, 523–548.

KIRÁLY, E. (1996): Adalékok a délkelet-dunántúli polimetamorf aljzat megismeréséhez. (Contributions to the recognition of the polymetamorphic basement of SE Transdanubia. in Hungarian).– Földtani Közlöny, 126/1, 1–23.

KLÖTZLI, U., BUDA, GY. & SKIÖLD, T. (2004): Zircon typology, geochronology and whole rock Sr-Nd isotope systematics of the Mecsek Mountain granitoids in the Tisia Terrane (Hungary).– Mineralogy and Petrology, 81, 113–134.

KOTKOVÁ, J. (2007): High-pressure granulites of the Bohemian Massif: recent advances and open questions.– Journal of Geosciences, 52, 45–71.

KOVÁCH, Á., SVINGOR, É. & SZEDERKÉNYI, T. (1985): Rb-Sr dating of basement rocks from the southern foreland of the Mecsek Mountains, Southern Transdanubia, Hungary.– Acta Mineralogica-Petrographica, Szeged XXVII, 51–56.

KOVÁCS, G., TÓTH, T.M. & SCHUBERT, F. (2009): A Gyódi Szerpentinit metamorf fejlődése. [*Metamorphic evolution of the Gyód serpentinite body – in Hungarian*].– In: TÓTH, T.M. (ed.): Magmás és metamorf képződmények a Tiszai Egységben. GeoLitera, 81–100.

LELKES-FELVÁRI, GY. & FRANK, W. (2006): Geochronology of the metamorphic basement, Transdanubian part of the Tisza Mega-Unit.– Acta Geologica Hungarica, 49/3, 189–206.

LE MAITRE, R.W. (1989): A Classification of Igneous Rocks and Glossary of Terms.– Blackwell, Oxford, 193 p.

MATTE, P.H., MALUSKI, H., RAJLICH, P. & FRANKE, W. (1990): Terrane boundaries in the Bohemian Massif: result of a large-scale Variscan shearing.– Tectonophysics, 177, 151–170.

MESCHEDE, M. (1986): A method of discriminating between different types of mid-ocean ridge basalts and continental tholeiites with a Nb-Zr-Y diagram.– Chemical Geology, 56, 207–218.

MEYRE, C., DE CAPITANI, C. & PARTZSCH, J.H. (1997): A ternary solid solution model for omphacite and its application to geothermobarometry of eclogites from the Middle Adula nappe (Central Alps, Switzerland).– Journal of Metamorphic Geology, 15, 687–700.

MORRISON, M.A. (1978): The use of "immobile" trace element to distinguish the paleotectonic affinities of metabasalts: applications to the paleocene basalts of Mull and Skye, northwest Scotland.– Earth and Planetary Science Letters, 39, 407–416.

NAGY, Á. & TÓTH, T.M. (2009): Relikt szöveti elemek a Görcsönyi Formáció óriásgránátos gneisz tagozat mintáiban [*Relict textures in the garnetiferous gneiss unit of the Görcsöny Formation – in Hungarian*].– In: TÓTH, T.M. (ed.): Magmás és metamorf képződmények a Tiszai Egységben. GeoLitera, 65–79.

NESBITT, H.W. & YOUNG, G.M. (1989): Formation and diagenesis of weathering profiles.– Journal of Geology, 97, 129–147.

O'BRIEN, P.J. (2000): The fundamental Variscan problem: high-temperature metamorphism at different depths and high-pressure metamorphism at different temperatures.– In: FRANKE, W., HAAK, V., ONCKEN, O. & TANNER, D. (eds.): Orogenic Processes: Quantification and modelling in the Variscan Belt, 369–386.

OGILVIE, P., GIBSON, R.L., REIMOLD, W.U. & DEUTSCH, A. (2004): Experimental investigation of schock effects in a metapelitic granulite.– 35th Lunar and Planetary Science Conference, March 15–19, 2004, League City, Texas, abstract no. 1242.

OLIVER, G.J.H., CORFU, F. & KROGH, T.E. (1993): U-Pb ages from SW Poland: evidence for a Caledonian suture zone between Baltica and Gondwana.– Journal of Geological Society, London, 150, 366–369.

PAMIĆ, J., BALEN, D. & TIBLJAŠ, D. (2002): Petrology and geochemistry of orthoamphibolites from the Variscan metamorphic sequences of the South Tisia in Croatia – an overview with geodynamic implications.– International Journal of Earth Sciences (Geologische Rundschau), 91, 787–798.

PEARCE, J.A. & CANN, J.R. (1973): Tectonic setting of basic volcanic rocks determined using trace element analyses.– Earth and Planetary Science Letters, 19, 290–300.

PEARCE, J.A. & GALE, G.H. (1977): Identification of ore-deposition environment from trace element geochemistry of associated igneous host rocks.– In: Volcanic processes in ore genesis; Geological Society London Publication, 7, 14–24.

PEARCE, J.A. & NORRY, M.J. (1979): Petrogenetic implications of Ti, Zr, Y and Nb variations in volcanic rocks.– Contributions to Mineralogy and Petrology, 69, 33–47.

PRAKASH, D., SINGH, P.C., ARIMA, M. & SINGH, T. (2012): P–T history and geochemical characteristics of mafic granulites and charnockites from west of Periya, North Kerala, southern India.– Journal of Asian Earth Sciences, 61, 102–115.

RAASE, P. (1974): Al and Ti contents of hornblende, indications of pressure and temperature of regional metamorphism.– Contributions to Mineralogy and Petrology, 45, 231–236.

RAGLAND, P.C., CONLEY, J.F., PARKER, W.C. & VAN ORMAN, J.A. (1997): Use of principal components analysis in petrology: an

example from the Martinsville igneous complex, Virginia, U.S.A.– Mineralogy and Petrology, 60, 165–184.

RAVASZ-BARANYAI, L. (1969): Eclogite from the Mecsek Mountains, Hungary.– Acta Geologica Academiae Scientiarum Hungaricae, 13, 315–322.

SAJEEV, K. & OSANAI, Y. (2004): Ultrahigh-temperature Metamorphism (1150 °C, 12 kbar) and Multistage Evolution of Mg-, Al-rich Granulites from the Central Highland Complex, Sri Lanka.– Journal of Petrology, 45/9, 1821–1844.

SUN, S.S. & MCDONOUGH, W.F. (1989): Chemical and isotopic systematics of oceanic basalts: implications for mantle composition and processes.– In: SAUNDERS, A.D. & NORRY, M. (eds): Magmatism in the Ocean Basins. Geological Society, London, Special Publications, 42*,* 313–*345.*

SZEDERKÉNYI, T. (1974): Paleozoic magmatism and tectogenesis in South-East Transdanubia.– Acta Geologica Academiae Scientiarum Hungaricae, 18, 305–313.

SZEDERKÉNYI, T. (1976): Barrow type metamorphism in the crystalline basement of Southeast Transdanubia.– Acta Geologica Academiae Scientiarum Hungaricae, 20/1–2, 47–61.

SZEDERKÉNYI, T. (1977): Geological evolution of South Transdanubia (Hungary) in Paleozoic time.– Acta Mineralogica-Petrographica, Szeged XXIII, 3–14.

SZEDERKÉNYI, T. (1983): Origin of amphibolites and metavolcanics of crystalline complexes of South Transdanubia, Hungary.– Acta Geologica Hungarica, 26/1–2, 103–136.

SZEDERKÉNYI, T. (1996): Metamorphic formations and their correlation in the Hungarian part of the Tisia megaunit (Tisia megaunit terrane).– Acta Mineralogica-Petrographica, Szeged XXXVII, 143–160.

TARNAI, T. (1997): Ore minerals from the key section of the Baksa Complex (W Baranya Hills, Hungary).– Acta Mineralogica-Petrographica, Szeged XXXVIII, Supplementum, 119–133.

TARNAI, T. (1998): Mineralogical-petrological study on ore vein penetrated by the key-borehole Baksa No. 2, SE Transdanubia, Hungary.– Acta Mineralogica-Petrographica, Szeged XXXIX, 21–34.

THOMPSON, R.N., DICKIN, A.P., GIBSON, I.L. & MORRISON, M.A. (1982): Elemental fingerprints of isotopic contamination of Hebridean Palaeocene mantle-derived magmas by Archean sial.– Contributions to Mineralogy and Petrology, 79, 159–168.

VAN DER MOLEN, I. & VAN ROERMUND, H.L.M. (1986): The pressure path of solid inclusions in minerals: the retention of coesite inclusion during uplift.– Lithos, 19, 317–324.

VON BLANCKENBURG, F. & DAVIES, J.H. (1995): Slab break-off: A model for syncollisional magmatism and tectonics in the Alps.– Tectonics, 14, 120–131.

WATERS, D.J. (2001): The significance of prograde and retrograde quartz-bearing intergrowth microstructures in partially melted granulite-facies rocks.– Lithos, 56, 97–110.

WHITNEY, D.L. & EVANS, B.W. (2010): Abbreviations for names of rock-forming minerals. – *American Mineralogist, 95, 185–187.*

WOOD, D.A. (1979): A variably veined suboceanic upper mantle genetic significance for mid-ocean ridge basalts from geochemical evidence.– Geology, 7, 499–503.

WOOD, D.A., GIBSON, I.L. & THOMPSON, R.N. (1976): Elemental mobility during zeolite facies metamorphism of the tertiary basalts of Eastern Iceland.– Contributions to Mineralogy and Petrology, 55, 241–254.

Manuscript received August 10, 2013
Revised manuscript accepted February 13, 2014
Available online March 21, 2014